Chemistry of Polynuclear Metal Complexes with Bridging Carbene or Carbyne Ligands. Part 86.[1] Alkylidyne(carbaborane)molybdenum–Gold, –Rhodium and –Iron Complexes; Crystal Structure of $[NEt_4][MoFe_2(\mu_3\text{-}CC_6H_4Me\text{-}4)(\mu\text{-}\sigma:\sigma':\eta^5\text{-}C_2B_9H_7Me_2)(CO)_8]$*

David D. Devore, Christiane Emmerich, Judith A. K. Howard, and F. Gordon A. Stone
Department of Inorganic Chemistry, The University, Bristol BS8 1TS

The alkylidyne–molybdenum complex $[NEt_4][Mo(\equiv CC_6H_4Me\text{-}4)(CO)\{P(OMe)_3\}(\eta^5\text{-}C_2B_9H_9Me_2)]$ has been prepared, and used to prepare compounds with bonds between molybdenum and gold, rhodium, and iron. Reactions of the molybdenum compound with $[AuCl(PPh_3)]$, $[Rh(cod)(PPh_3)_2][PF_6]$ (cod = cyclo-octa-1,5-diene), and $[Fe_2(CO)_9]$ afford, respectively, the complexes $[MoAu(\mu\text{-}CC_6H_4Me\text{-}4)(CO)\{P(OMe)_3\}(PPh_3)(\eta^5\text{-}C_2B_9H_9Me_2)]$, $[MoRh(\mu\text{-}CC_6H_4Me\text{-}4)(\mu\text{-}CO)\{P(OMe)_3\}(PPh_3)_2(\eta^5\text{-}C_2B_9H_9Me_2)]$, and $[NEt_4][MoFe_2(\mu_3\text{-}CC_6H_4Me\text{-}4)(\mu\text{-}\sigma:\sigma':\eta^5\text{-}C_2B_9H_7Me_2)(CO)_8]$. The structure of the latter has been established by *X*-ray diffraction. There are two crystallographically independent anions with their associated cations in the asymmetric unit but with overall very similar geometries. In the anions a triangle of metal atoms is symmetrically capped on one side by the alkylidyne ligand. On the other side of the triangle the molybdenum atom is η^5-ligated by the C_2B_9 cage, but two boron atoms in the pentagonal face are σ bonded to the two iron atoms. The molybdenum carries two carbonyl groups and each of the iron atoms is bonded by three of these ligands. The reaction between $[Fe_2(CO)_9]$ and $[NEt_4][Mo(\equiv CC_6H_4Me\text{-}4)(CO)\{P(OMe)_3\}(\eta^5\text{-}C_2B_9H_9Me_2)]$ also affords the novel mononuclear molybdenum compound $[NEt_4][Mo\{\sigma,\eta^5\text{-}CH(C_6H_4Me\text{-}4)C_2B_9H_8Me_2\}(CO)_3]$. Protonation ($HBF_4{\cdot}Et_2O$) of CO-saturated CH_2Cl_2 solutions of the latter gives the neutral complex $[Mo(CO)_4\{\eta^5\text{-}C_2B_9H_8(CH_2C_6H_4Me\text{-}4)Me_2\}]$. Protonation in the presence of an excess of PMe_3 gives a mixture of the two compounds $[Mo(CO)_3(L)\{\eta^5\text{-}C_2B_9H_8(CH_2C_6H_4Me\text{-}4)Me_2\}]$ (L = PMe_3 or CO). The n.m.r. data (^1H, $^{13}C\text{-}\{^1H\}$, $^{11}B\text{-}\{^1H\}$, and $^{31}P\text{-}\{^1H\}$) for the new compounds are reported and discussed.

The $[N(PPh_3)_2]^+$, $[NEt_4]^+$, $[P(CH_2Ph)Ph_3]^+$, or $[PPh_4]^+$ salts of the anionic complexes $[W(\equiv CR)(CO)_2(\eta^5\text{-}C_2B_9H_9Me_2)]^-$ [R = Me (**1a**), Ph (**1b**), C_6H_4Me-4 (**1c**), C_6H_4Me-2 (**1d**), or $C_6H_3Me_2$-2,6 (**1e**)] have proven to be versatile reagents for preparing di- or tri-metal compounds in which the metal–metal bonds are bridged by alkylidyne ligands.[2] Moreover, in many of the products the carbaborane ligand adopts a non-spectator role, a feature which may take a variety of forms. The most common modification of the carbaborane group involves slippage away from the tungsten so as to form an exopolyhedral B–H→metal bond with an adjacent metal atom. This is accomplished using a BH group in the pentagonal face of the icosahedral $C_2B_9H_9Me_2$ fragment while the latter remains η^5-co-ordinated to tungsten. Further transformations can occur, leading to formation of exopolyhedral boron–metal σ bonds. Moreover, in some reactions novel modifications of the alkylidyne ligand are also observed. Hence it has become apparent that species in which the metal–metal bonds are bridged both by alkylidyne ligands and by exopolyhedral B–H→metal linkages are often intermediates for further reactions.[2e–i,3] Thus treatment of the $[N(PPh_3)_2]^+$ salt of (**1c**) with $[Mo(CO)_2(NCMe)_2(\eta^5\text{-}C_9H_7)][BF_4]$ (C_9H_7 = indenyl) affords the dimetal compound $[MoW(\mu\text{-}CC_6H_4Me\text{-}4)(CO)_3(\eta^5\text{-}C_9H_7)(\eta^5\text{-}C_2B_9H_9Me_2)]$ (**2**).[2c] The latter reacts with hex-3-yne to produce $[MoW\{\mu\text{-}\sigma:\eta^5\text{-}CH(C_6H_4Me\text{-}4)C_2B_9H_8Me_2\}(CO)_3(\eta\text{-}EtC_2Et)(\eta^5\text{-}C_9H_7)]$ (**3**), containing an unusual

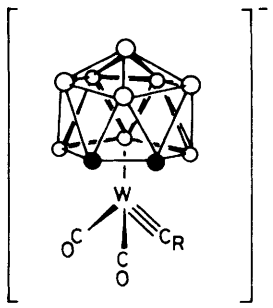

R

(**1a**) Me
(**1b**) Ph
(**1c**) C_6H_4Me-4
(**1d**) C_6H_4Me-2
(**1e**) $C_6H_3Me_2$-2,6

B–$CH(C_6H_4Me\text{-}4)$–Mo bridge system.[3a] A similar bridge system involving ruthenium exists in $[WRu\{\mu\text{-}\sigma:\eta^5\text{-}CH(C_6H_4Me\text{-}4)C_2B_9H_8Me_2\}(CO)_3(PMe_3)(\eta\text{-}C_5H_5)]$ (**4**), obtained by treating $[WRu(\mu\text{-}CC_6H_4Me\text{-}4)(CO)_3(\eta\text{-}C_5H_5)(\eta^5\text{-}C_2B_9H_9Me_2)]$ (**5**) with PMe_3.[2b] An especially novel transformation of the alkylidyne ligand occurs in the reaction between the $[N(PPh_3)_2]^+$ salt of (**1c**) and $[PtH(Me_2CO)(PEt_3)_2][BF_4]$. The product, $[WPt(CO)_2(PEt_3)_2\{\eta^6\text{-}C_2B_9H_8(CH_2C_6H_4Me\text{-}4)Me_2\}]$ (**6**), is a species in which the carbaborane cage carries a $CH_2C_6H_4Me$-4 substituent. Moreover, the carbon atoms in the

* 1,1,1,2,2,2,3,3-Octacarbonyl-μ-[σ:σ′:η⁵-7,8-dimethyl-7,8-dicarbaundecaborato-*B*⁷⁻¹¹ (Mo³), *B*⁹(Fe²),*B*¹⁰(Fe¹)]-μ₃-*p*-tolylmethylidyne-*triangulo*-di-ironmolybdenum.

Supplementary data available: see Instructions for Authors, *J. Chem. Soc., Dalton Trans.*, 1989, Issue 1, pp. xvii–xx.

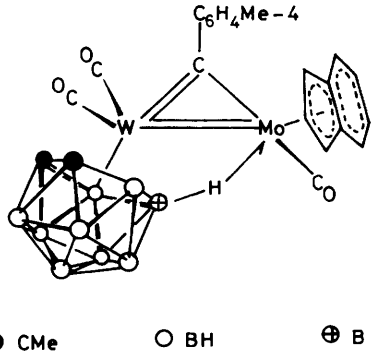

(2)

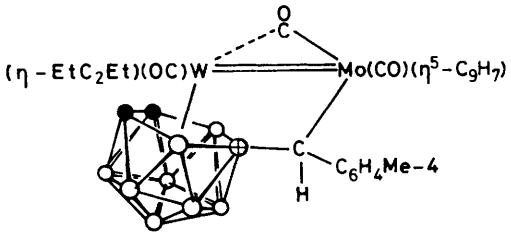

(3)

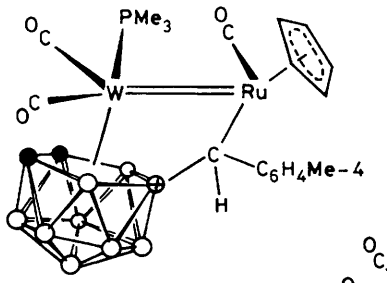

(4)

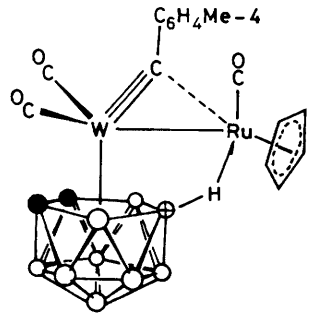

(5)

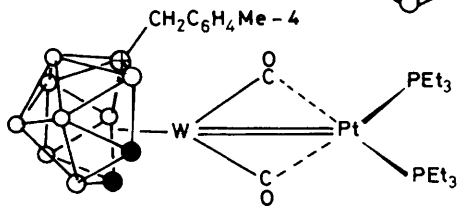

(6)

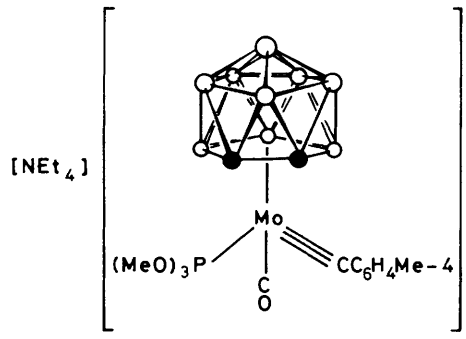

(7)

face of the carbaborane fragment are non-bonding, being 2.88 Å apart.[2e]

Recent work has revealed significant differences in reactivity patterns between the tungsten and molybdenum complexes $[M(\equiv CR)(CO)_2(\eta\text{-}C_5H_5)]$ (M = Mo or W, R = alkyl or aryl) in their respective reactions with low-valent metal fragments.[4] It therefore seemed desirable, for comparative purposes, to study reactions of molybdenum complexes akin to (**1**), and in this paper we report the synthesis of $[NEt_4][Mo(\equiv CC_6H_4Me\text{-}4)(CO)\{P(OMe)_3\}(\eta^5\text{-}C_2B_9H_9Me_2)]$ (**7**), and its reactions with $[AuCl(PPh_3)]$, $[Rh(cod)(PPh_3)_2][PF_6]$ (cod = cyclo-octa-1,5-diene), and $[Fe_2(CO)_9]$.

Results and Discussion

The reaction between $Na_2[7,8\text{-}C_2B_9H_9Me_2]$, generated *in situ* from $[NHMe_3][7,8\text{-}C_2B_9H_{10}Me_2]$ and NaH in thf (tetrahydrofuran), and $[Mo(\equiv CC_6H_4Me\text{-}4)Cl(CO)\{P(OMe)_3\}_3]$, followed by addition of $[NEt_4]Cl$, affords the salt $[NEt_4][Mo(\equiv CC_6H_4Me\text{-}4)(CO)\{P(OMe)_3\}(\eta^5\text{-}C_2B_9H_9Me_2)]$ (**7**). Data for this red crystalline solid are given in Tables 1—3. The i.r. spectrum shows a broad, moderately strong B–H stretch at 2 528 cm^{-1}, and a single strong CO band at 1 872 cm^{-1}. In the $^{13}C\text{-}\{^1H\}$ n.m.r. spectrum (Table 2), the resonance at δ 293.8 p.p.m., a doublet with $^{31}P\text{–}^{13}C$ coupling (34 Hz), confirms the presence of the alkylidyne group. Salts of the anionic complexes (**1**) all show alkylidyne carbon resonances in their $^{13}C\text{-}\{^1H\}$ n.m.r. spectra near 300 p.p.m.[2a,f] The spectrum of (**7**) also has a single CO resonance at δ 244.3 p.p.m., appearing as a doublet due to coupling (22 Hz) with the $^{31}P(OMe)_3$ ligand. Other signals in the $^{13}C\text{-}\{^1H\}$ n.m.r. spectrum are readily assigned (Table 2). In the $^{31}P\text{-}\{^1H\}$ n.m.r. spectrum, the resonance for the $P(OMe)_3$ group is a singlet at δ 194.0 p.p.m., while the $^{11}B\text{-}\{^1H\}$ n.m.r. spectrum (Table 3) shows four broad unresolved signals.

Treatment of a thf solution of (**7**) with one equivalent of $[AuCl(PPh_3)]$, in the presence of KPF_6, to facilitate removal of chloride, affords the red compound $[MoAu(\mu\text{-}CC_6H_4Me\text{-}4)(CO)\{P(OMe)_3\}(PPh_3)(\eta^5\text{-}C_2B_9H_9Me_2)]$ (**8a**), characterised by the data given in Tables 1—3. We have previously reported[2a] the related tungsten–gold complex $[WAu(\mu\text{-}CC_6H_4Me\text{-}4)(CO)_2(PPh_3)(\eta^5\text{-}C_2B_9H_9Me_2)]$ (**8b**), prepared by treating the $[N(PPh_3)_2]^+$ salt of (**1c**) with $[AuCl(PPh_3)]$, in the presence of $TlPF_6$.

The $^{31}P\text{-}\{^1H\}$ n.m.r. spectrum of (**8a**) (Table 3) showed characteristic peaks for the $P(OMe)_3$ and PPh_3 ligands. The $^{11}B\text{-}\{^1H\}$ n.m.r. spectrum was less informative showing only one broad band, but this is not unusual for dimetal compounds in which the $\eta^5\text{-}C_2B_9H_9Me_2$ ligand does not engage in exopolyhedral bonding. In the $^{13}C\text{-}\{^1H\}$ n.mr. spectrum of (**8a**) the μ-C group resonates at δ 289.6 p.p.m. The signal was an apparent triplet [J(PC) 28 Hz] resulting from overlapping doublets, arising from ^{31}P coupling with the $P(OMe)_3$ and PPh_3 ligands. The μ-C resonance in the spectrum of (**8b**) is at δ 292.9 p.p.m., a doublet with J(PC) 28 Hz. An X-ray diffraction study[2a] on (**8b**) revealed that the p-tolylmethylidyne ligand asymmetrically bridges the W–Au bond. Indeed, the W–μ-C–$C^1(C_6H_4Me\text{-}4)$ angle of 163(2)°, and the short W–μ-C distance [1.88(3) Å], indicate that bonding of the $Au(PPh_3)$ group to the $W{\equiv}CC_6H_4Me\text{-}4$ fragment has had little effect on the geometry of the latter. Asymmetric $\mu\text{-}CC_6H_4Me\text{-}4$ bridging

Table 1. Analytical[a] and physical data for the complexes

	Compound	Colour	Yield (%)	$\nu_{max.}$(CO)[b]/cm^{-1}	Analysis (%) C	H
(7)	$[NEt_4][Mo(\equiv CC_6H_4Me\text{-}4)(CO)\{P(OMe)_3\}(\eta^5\text{-}C_2B_9H_9Me_2)]$	Red	54	1 872s	[c]44.5 (44.9)	8.7 (8.0)
(8a)	$[MoAu(\mu\text{-}CC_6H_4Me\text{-}4)(CO)\{P(OMe)_3\}(PPh_3)(\eta^5\text{-}C_2B_9H_9Me_2)]$	Red	48	1 923s	41.6 (42.1)	5.1 (4.8)
(9a)	$[MoRh(\mu\text{-}CC_6H_4Me\text{-}4)(\mu\text{-}CO)\{P(OMe)_3\}(PPh_3)_2(\eta^5\text{-}C_2B_9H_9Me_2)]$	Brown	55	1 737m	54.2 (54.8)	5.5 (5.4)
(10a)	$[NEt_4][MoFe_2(\mu_3\text{-}CC_6H_4Me\text{-}4)(\mu\text{-}\sigma\text{:}\sigma'\text{:}\eta^5\text{-}C_2B_9H_7Me_2)(CO)_8]$	Copper-brown	21[d]	2 031m, 1 985vs, 1 958m, 1 945 (sh), 1 932 (sh)	[e]40.9 (40.8)	5.1 (4.9)
(11)	$[NEt_4][Mo\{\sigma,\eta^5\text{-}CH(C_6H_4Me\text{-}4)C_2B_9H_8Me_2\}(CO)_3]$	Brown	30[d]	1 964vs, 1 865m		
(13a)	$[Mo(CO)_3(PMe_3)\{\eta^5\text{-}C_2B_9H_8(CH_2C_6H_4Me\text{-}4)Me_2\}]$	Tan	13	[f]2 028s, 1 963m, 1 924vs	41.2 (41.5)	6.4 (6.2)
(13b)	$[Mo(CO)_4\{\eta^5\text{-}C_2B_9H_8(CH_2C_6H_4Me\text{-}4)Me_2\}]$	Tan	20	[f]2 093vs, 2 034m, 2 001s(br)	41.1 (40.7)	5.2 (4.9)
(14)	$[MoFe_2(\mu\text{-}H)(\mu_3\text{-}CC_6H_4Me\text{-}4)(\mu\text{-}\sigma\text{:}\sigma'\text{:}\eta^5\text{-}C_2B_9H_7Me_2)(CO)_8]$	Yellow-brown	70	[f]2 083m, 2 057s, 2 033m, 2 017vs, 1 996w, 1 967w	34.3 (34.6)	3.6 (3.1)

[a] Calculated values are given in parentheses. [b] In CH_2Cl_2; in the spectra of all the complexes a broad band due to BH is observed in the range 2 575—2 528 cm^{-1}. [c] N, 2.7 (2.2%). [d] Estimated from relative intensity of peaks in ^{1}H n.m.r. spectrum of mixture, see Experimental section. [e] N, 2.1 (1.7%). [f] In Et_2O.

Table 2. Hydrogen-1 and carbon-13 n.m.r. data[a] for the complexes

Compound	^{1}H[b,c](δ)	^{13}C[d](δ)
(7)	1.26 [t of t, 12 H, NCH_2Me, *J*(HH) 7, *J*(NH) 2], 1.83, 2.10, 2.26 (s × 3, 9 H, CMe, Me-4), 3.14 [q, 8 H, NCH_2Me, *J*(HH) 7], 3.70 [d, 9 H, OMe, *J*(PH) 12], 7.02, 7.36 [$(AB)_2$, 4 H, C_6H_4, *J*(AB) 8]	293.8 [d, C≡Mo, *J*(PC) 34], 244.3 [d, CO, *J*(PC) 22], 145.8 [C^1(C_6H_4)], 137.2, 128.8, 128.6 (C_6H_4), 78.0, 60.7 (br, *C*Me), 53.1 (NCH_2Me), 51.8 (OMe), 30.4, 28.2 (*CMe*), 21.7 (Me-4), 7.8 (NCH_2Me)
(8a)	1.84, 2.17, 2.35 (s × 3, 9 H, CMe, Me-4), 3.69 [d, 9 H, OMe, *J*(PH) 11], 7.09, 7.56 [$(AB)_2$, 4 H, C_6H_4, *J*(AB) 8], 7.46 (m, 15 H, Ph)	[e]289.6 [t, μ-C, *J*(PC) 28], 240.8 [d, CO, *J*(PC) 27], 147.5 [C^1(C_6H_4)], 140.2 (C_6H_4), 135.4 [d, Ph, *J*(PC) 15], 132.3 (Ph), 129.7 [d, Ph, *J*(PC) 11], 129.4, 129.1 (C_6H_4), 67.7, 67.1 (br, *C*Me), 31.9, 29.1 (*CMe*), 21.8 (Me-4)
(9a)	1.50, 2.14, 2.43 (s × 3, 9 H, CMe, Me-4), 3.04 [d, 9 H, OMe, *J*(PH) 11], 6.96—7.42 (m, 34 H, C_6H_4, Ph)	[e]333.7 (m, μ-C), 268.7 [d of d, μ-CO, *J*(PC) 15, *J*(RhC) 32], 150.9 [C^1(C_6H_4)], 138.5 (C_6H_4), 135.0, 134.2 [d × 2, Ph, *J*(PC) 12, 11], 130.4, 130.3 (Ph), 128.8, 128.6 (C_6H_4), 128.4, 128.3, 128.2 (Ph), 67.5, 66.8 (br, *C*Me), 28.1, 27.1 (*CMe*), 21.9 (Me-4)
(10a)	1.31 [t, 12 H, NCH_2Me, *J*(HH) 6], 2.07, 2.21, 2.39 (s × 3, 9 H, CMe, Me-4), 3.15 [q, 8 H, NCH_2Me, *J*(HH) 7], 7.13, 7.32 [$(AB)_2$, 4 H, C_6H_4, *J*(AB) 8]	314.0 (μ_3-C), 232.1, 226.8 (MoCO), 216.2, 215.8 (FeCO), 158.4 [C^1(C_6H_4)], 134.9, 128.0, 127.6 (C_6H_4), 62.5, 55.8 (br, *C*Me), 53.2 (NCH_2Me), 32.6, 31.4 (*CMe*), 21.3 (Me-4), 7.9 (NCH_2Me)
(11)	1.22 (m, br, 12 H, NCH_2Me), 1.99, 2.00, 2.23 (s × 3, 9 H, CMe, Me-4), 3.03 [q, 8 H, NCH_2Me, *J*(HH) 7], 5.10 [s, 1 H, *CH*(C_6H_4Me-4)], 6.94, 7.26 [$(AB)_2$, 4 H, C_6H_4, *J*(AB) 8]	233.0 (CO), 147.7 [C^1(C_6H_4)], 134.0, 128.8, 128.3 (C_6H_4), 80.0 [br, *C*H(C_6H_4Me-4)], 72.3, 59.0 (*C*Me), 53.5 (NCH_2Me), 31.5, 31.0 (*CMe*), 21.3 (Me-4), 7.8 (NCH_2Me)
(13a)	1.92 [d, 9 H, MeP, *J*(PH) 10], 2.15 [s, br, 2 H, CH_2(C_6H_4Me-4)], 2.20 (s, 6 H, CMe), 2.22 (s, 3 H, Me-4), 6.73, 6.90 [$(AB)_2$, 4 H, C_6H_4, *J*(AB) 8]	228.9, 228.6 (CO), 144.2 [C^1(C_6H_4)], 132.9, 129.2, 128.1 (C_6H_4), 71.2 (br, *C*Me), 33.0 [v br, CH_2(C_6H_4Me-4)], 32.2 (*CMe*), 21.0 (Me-4), 17.8 [d, MeP, *J*(PC) 35]
(13b)	2.18 [s br, 2 H, CH_2(C_6H_4Me-4)], 2.24 (s, 6 H, CMe), 2.26 (s, 3 H, Me-4), 6.88, 6.97 [$(AB)_2$, 4 H, C_6H_4, *J*(AB) 7]	220.3 (CO), 142.9 [C^1(C_6H_4)], 134.3, 129.1, 128.8 (C_6H_4), 75.5 (br, *C*Me), 33.3 (*CMe*), 32.6 [v br, CH_2(C_6H_4Me-4)], 21.0 (Me-4)
(14)	[f] −24.98 (s, 1 H, μ-H), 2.19, 2.23, 2.41 (s × 3, 9 H, CMe, Me-4), 7.22, 7.30 [$(AB)_2$, 4 H, C_6H_4, *J*(AB) 8]	[f]312.6 (μ_3-C), 226.3, 223.3 (MoCO), 210.8, 210.5, 207.3, 206.8, 206.3, 203.5 (FeCO), 156.1 [C^1(C_6H_4)], 138.3, 129.3, 126.2 (C_6H_4), 66.8, 55.9 (br, *C*Me), 32.0, 31.5 (*CMe*), 21.3 (Me-4)
	[g] −26.83 (s, 1 H, μ-H), 2.14 (s, 3 H, CMe)	[g]312.4 (μ_3-C), 224.7, 223.0 (MoCO), 212.6, 210.2, 207.5, 206.5, 205.1 (FeCO), 155.9 [C^1(C_6H_4)], 126.5 (C_6H_4), 34.4 (*CMe*)

[a] Chemical shifts (δ) in p.p.m., coupling constants in Hz. Measurements at ambient temperatures. [b] Measured in CD_2Cl_2. [c] Proton resonances for the BH groups occur as broad unresolved signals in the range δ 0—3. [d] Hydrogen-1 decoupled, chemical shifts are positive to high frequency of $SiMe_4$, with measurements in CD_2Cl_2—CH_2Cl_2. [e] Signal for PO*Me* group obscured by solvent peak. [f] Peaks for major isomer. [g] Peaks for minor isomer, other signals obscured by signals for major isomers.

is likely to be present in (**8a**) also, since the μ-C resonances in the ^{13}C-{^{1}H} n.m.r. spectra of the two complexes are so similar and are close to that observed (δ 293.8 p.p.m.) for the terminal Mo≡C group in (**7**). In dimetal complexes with bridging alkylidyne groups the signals for the μ-C nuclei are generally significantly more deshielded than 300 p.p.m.[4d,5]

Compound (**8a**) appears to be more stable than (**8b**). In the synthesis of the latter a by-product was the salt $[N(PPh_3)_2][W_2Au(\mu\text{-}CC_6H_4Me\text{-}4)_2(CO)_4(\eta^5\text{-}C_2B_9H_9Me_2)_2]$, formed by displacement of the PPh_3 group in (**8b**) by the C≡W moiety of (**1c**). No similar trimetal species was observed to form in the reaction between $[AuCl(PPh_3)]$ and (**7**).

The reaction between (**7**) and $[Rh(cod)(PPh_3)_2][PF_6]$ in CH_2Cl_2 afforded the compound $[MoRh(\mu\text{-}CC_6H_4Me\text{-}4)(\mu\text{-}CO)\{P(OMe)_3\}(PPh_3)_2(\eta^5\text{-}C_2B_9H_9Me_2)]$ (**9a**), data for which are summarised in Tables 1—3. The related tungsten–rhodium compound $[WRh(\mu\text{-}CC_6H_4Me\text{-}4)(\mu\text{-}CO)(CO)(PPh_3)_2(\eta^5\text{-}C_2B_9H_9Me_2)]$ (**9b**) has been prepared by treating the $[N(PPh_3)_2]^+$ salt of (**1c**) with $[RhCl(PPh_3)_3]$ or $[Rh(cod)(PPh_3)_2][PF_6]$. An *X*-ray diffraction study revealed that it contained a strongly

Table 3. Boron-11 and phosphorus-31 n.m.r. data[a] for the complexes

Compound	^{11}B[b](δ)	^{31}P[c](δ)
(7)	−11.7, −20.2, −36.8, −38.7 (9 B)	194.0 [s, $P(OMe)_3$]
(8a)	−8.8 (br, 9 B)	173.7 [s, $P(OMe)_3$], 50.8 (s, PPh_3)
(9a)	−10.0 (br, 9 B)	174.2 [d of d, $P(OMe)_3$, *J*(PP) 31, 11], 38.0 [d of d of d, PPh_3, *J*(PP) 46, 31; *J*(RhP) 186], 28.8 [d of d of d, PPh_3, *J*(PP) 45, 11; *J*(RhP) 156]
(10a)	59.0, 47.8 (2 B, BFe), −2.9 (1 B), −5.0 (1 B), −6.9 (1 B), −10.3 (2 B), −14.3 (2 B)	
(11)	8.7 (1 B, BC), −5.4 (1 B), −7.5 (1 B), −8.5 (2 B), −13.1 (2 B), −14.6 (1 B), −16.1 (1 B)	
(13a)	9.7 (1 B, $BCH_2C_6H_4Me$-4), −4.0 (1 B), −4.9 (3 B), −6.8 (2 B), −9.3 (2 B)	12.2 (s, PMe_3)
(13b)	13.4 (1 B, $BCH_2C_6H_4Me$-4), 1.0 (1 B), −1.6 (2 B), −5.8 (2 B), −7.0 (3 B)	
(14)[d]	58.7, 46.2 (2 B, BFe), −0.7 (1 B), −3.0 (1 B), −7.4 (1 B), −8.5 (1 B), −9.9 (1 B), −11.4 (2 B)	

[a] Chemical shifts (δ) in p.p.m., coupling constants in Hz. Measurements at room temperature in CD_2Cl_2–CH_2Cl_2. [b] Hydrogen-1 decoupled, chemical shifts are positive to high frequency of BF_3·Et_2O (external). [c] Hydrogen-1 decoupled, chemical shifts are positive to high frequency of 85% H_3PO_4 (external). [d] Peaks are for major isomer, see text.

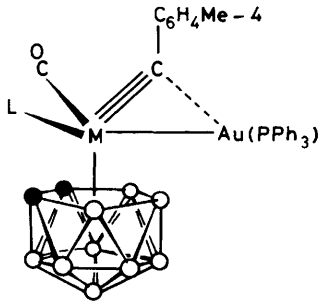

	M	L
(8a)	Mo	$P(OMe)_3$
(8b)	W	CO

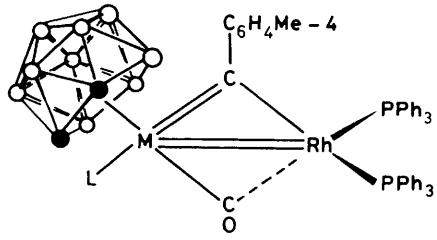

	M	L
(9a)	Mo	$P(OMe)_3$
(9b)	W	CO

semi-bridging CO ligand.[2a] Moreover, in solution, the i.r. spectrum showed a CO absorption at 1 767 cm^{-1}, implying that under these conditions the carbonyl group in (**9b**) might even be fully bridging. The corresponding band in the i.r. spectrum of (**9a**) is at lower frequency (1 737 cm^{-1}). In the ^{13}C-{^1H} n.m.r. spectrum (Table 2), (**9a**) shows a μ-CO resonance at δ 268.7 p.p.m. [*J*(PC) 15 and *J*(RhC) 32 Hz]. The ^{13}C-^{103}Rh coupling is larger than that observed (17 Hz) on the μ-CO resonance (δ 236.1 p.p.m.) in the spectrum of (**9b**) and this, together with the more deshielded chemical shift, suggests that in (**9a**) the carbonyl group is fully bridging. The bridge-system in (**9a**), therefore, may be best represented by (**A'**) rather than (**B'**), below.

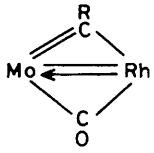

(**A'**)

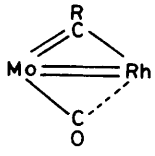

(**B'**)

In the ^{13}C-{^1H} n.m.r. spectrum of (**9a**) the μ-C nucleus resonates at δ 333.7 p.p.m. The signal is an unresolved multiplet due to ^{31}P and ^{103}Rh coupling. In the spectrum of (**9b**) the alkylidyne carbon peak is a doublet [*J*(RhC) 30 Hz] at δ 343.1 p.p.m.

The ^{13}C-{^1H} and ^{31}P-{^1H} n.m.r. data[2a] for (**9b**) revealed that this species underwent dynamic behaviour in solution, involving both site exchange of the bridging and terminal CO groups and rotation of the $Rh(PPh_3)_2$ group. Compound (**9a**) shows no PPh_3 exchange process at room temperature. The ^{31}P-{^1H} n.m.r. spectrum (Table 3) shows a signal for each of the non-equivalent PPh_3 ligands with an ABMX pattern. In addition, there is the expected signal for the $P(OMe)_3$ ligand, appearing as a doublet of doublets due to coupling with the two PPh_3 groups. The ^{11}B-{^1H} n.m.r. spectrum (Table 3) shows one broad band, as expected for the proposed structure in which the carbaborane group is not involved in exopolyhedral bonding.

The reaction between (**7**) and $[Fe_2(CO)_9]$ was next investigated, since reactions between iron carbonyls and the $[NEt_4]^+$ salts of (**1**) had been investigated earlier.[2g,h] In thf at room temperature, mixtures of (**7**) and $[Fe_2(CO)_9]$ afforded the two complexes $[NEt_4][MoFe_2(\mu_3\text{-}CC_6H_4Me\text{-}4)(\mu\text{-}\sigma\text{:}\sigma'\text{:}\eta^5\text{-}C_2B_9H_7Me_2)(CO)_8]$ (**10a**) and $[NEt_4][Mo\{\sigma,\eta^5\text{-}CH(C_6H_4\text{-}Me\text{-}4)C_2B_9H_8Me_2\}(CO)_3]$ (**11**), the characterisation of which is described below. Formation of (**10a**) was not surprising since in the earlier work the related compound $[NEt_4][WFe_2(\mu_3\text{-}CC_6H_4Me\text{-}4)(\mu\text{-}\sigma\text{:}\sigma'\text{:}\eta^5\text{-}C_2B_9H_7Me_2)(CO)_8]$ was obtained by treating the $[NEt_4]^+$ salt of (**1c**) with $[Fe_2(CO)_9]$.[2g] Another product of this reaction, however, was the dimetal compound $[NEt_4][WFe\{\mu\text{-}CH(C_6H_4Me\text{-}4)\}(\mu\text{-}\sigma\text{:}\eta^5\text{-}C_2B_9H_8Me_2)(\mu\text{-}CO)(CO)_5]$ (**12**). No analogue of the latter complex was observed in the reaction between (**7**) and $[Fe_2(CO)_9]$.

As described in the Experimental section, it was difficult to separate (**10a**) from (**11**), and hence microanalytical data on the latter species were not obtained. However, derivatives of (**11**) were prepared and fully characterised, as described below. The compounds (**10a**) and (**11**) were formed in approximately equal amounts, as deduced from integration of peaks in the ^1H n.m.r.

spectra of the initially formed mixture. Minor reaction products were $[Fe_3(CO)_{12}]$ and $[NEt_4][Fe_3(\mu\text{-}H)(CO)_{11}]$, but these by-products are also formed in the synthesis of (**10b**) and (**12**). Neither (**10a**) nor (**11**) contained a $P(OMe)_3$ group, as became obvious from n.m.r. studies. Presumably this ligand is removed in the reaction as $[Fe(CO)_4\{P(OMe)_3\}]$. However, the latter was not identified, probably being removed with the solvent on pumping. Data for (**10a**) and (**11**) are given in Tables 1—3.

Examination of the $^{13}C\text{-}\{^1H\}$ n.m.r. spectrum of (**10a**) did not initially resolve its structure. Resonances at δ 232.1 and 226.8 p.p.m. could be assigned to the $Mo(CO)_2$ group. However, only two FeCO peaks (δ 216.2 and 215.8 p.p.m.) were observed. In contrast, the $^{13}C\text{-}\{^1H\}$ n.m.r. spectrum of (**10b**) shows four FeCO signals.[2g] More significantly the μ_3-C resonance in (**10a**) occurs at δ 314.0 p.p.m., whereas in (**10b**) it is seen at δ 271.8 p.p.m. The latter signal is in the normal range for an alkylidyne group triply bridging three metal atoms, while the former peak has a chemical shift more in the region for an alkylidyne group spanning two metal centres.[4d,5,6] However, compounds in which the alkylidyne ligand asymmetrically caps a metal triangle have n.m.r. shifts for the ligated carbon atom near δ 300 p.p.m. In order to establish firmly the structure of (**10a**) an *X*-ray diffraction study was carried out. There are two crystallographically independent anions with their associated cations in the asymmetric unit. The anions have similar overall geometries but with different configurations of the carbaborane cage with respect to the metal atom triangle, as shown below. In each anion one carbonyl ligand on the Mo atom virtually eclipses a C–Me vector, but these C–Me bonds adopt different orientations with respect to the metal triangle. Selected bond distances and angles for both anions are listed in Table 4. The structure of the anion of molecule 1 is shown in the Figure and the discussion below relates to this molecule.

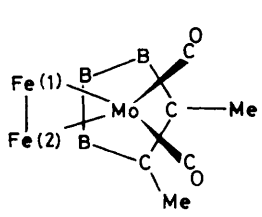

Anion (1)

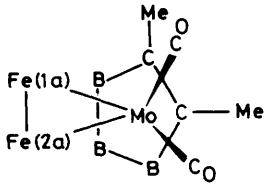

Anion (2)

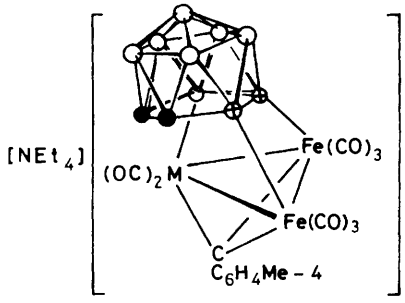

M

(**10a**) Mo

(**10b**) W

It is immediately apparent that the metal triangle [Mo–Fe(1) 2.643(2), Mo–Fe(2) 2.619(2), Fe(1)–Fe(2) 2.590(3) Å] is capped by the *p*-tolylmethylidyne ligand [C(1)–Mo 2.02(1), C(1)–Fe(1) 2.04(1), C(1)–Fe(2) 2.02(2) Å]. This group is thus symmetrically disposed with respect to the three metal atoms. Hence the relatively deshielded $^{13}C\text{-}\{^1H\}$ n.m.r. resonance observed for C(1) must be due either to it being bonded to a molybdenum atom, or to the molecule adopting a less symmetrical structure in solution. Replacement of tungsten atoms by molybdenum atoms in polynuclear metal complexes with bridging alkylidyne ligands leads to the ^{13}C n.m.r. resonances for these groups becoming more deshielded.[1] However, the increased deshielding is in general not so pronounced as the Δδ of *ca.* 42 p.p.m. shown between (**10a**) and (**10b**).

The structure of the anion of (**10a**) is very similar to that of $[WFe_2(\mu_3\text{-}CPh)(\mu\text{-}\sigma\text{:}\sigma'\text{:}\eta^5\text{-}C_2B_9H_7Me_2)(CO)_8]^-$.[2g] As in the latter, the carbaborane cage in (**10a**) has slipped over the $MoFe_2$ core, on the opposite side to the $\mu_3\text{-}CC_6H_4Me\text{-}4$ group, so as to form two boron–iron σ bonds [B(1)–Fe(2) and B(2)–Fe(1) 2.12(2) Å]. The carbaborane cage thus formally donates a total of six valence electrons to the cluster anion, which overall is a 48 valence-electron species. The molybdenum atom, apart from the

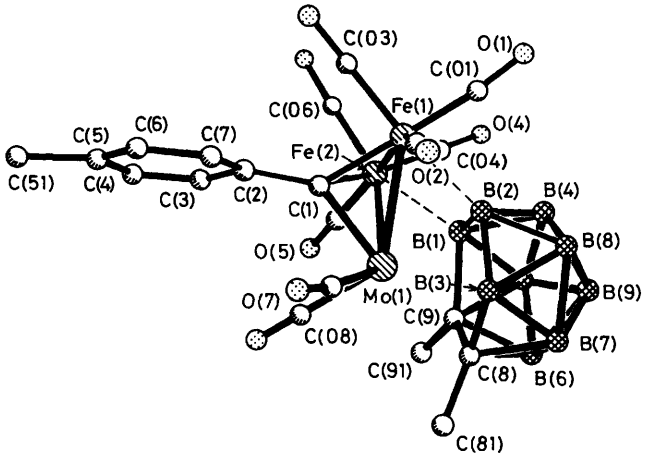

Figure. Structure of the anion (1) of the salt $[NEt_4][MoFe_2(\mu_3\text{-}CC_6H_4Me\text{-}4)(\mu\text{-}\sigma\text{:}\sigma'\text{:}\eta^5\text{-}C_2B_9H_7Me_2)(CO)_8]$ (**10a**) showing the crystallographic numbering scheme

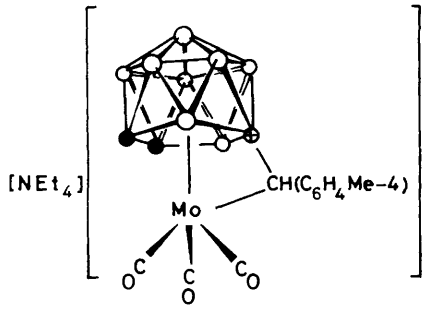

(**11**)

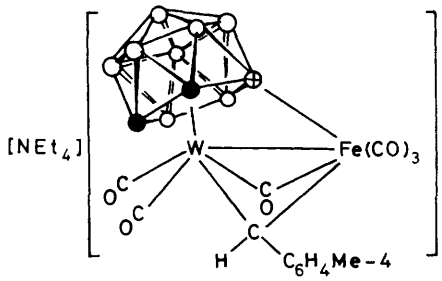

(**12**)

Table 4. Selected internuclear distances (Å) and angles (°) for the complex $[NEt_4][MoFe_2(\mu_3\text{-}CC_6H_4Me\text{-}4)(\mu\text{-}\sigma:\sigma':\eta^5\text{-}C_2B_9H_7Me_2)(CO)_8]$ (**10a**)

Anion 1		Anion 2		Anion 1		Anion 2	
Mo–Fe(1)	2.643(2)	Mo(a)–Fe(1a)	2.642(2)	Mo–Fe(2)	2.619(2)	Mo(a)–Fe(2a)	2.644(2)
Mo–C(07)	2.03(2)	Mo(a)–C(07a)	2.08(2)	Mo–C(08)	2.02(2)	Mo(a)–C(08a)	2.02(1)
Mo–C(1)	2.02(1)	Mo(a)–C(1a)	2.04(1)	Mo–B(1)	2.21(2)	Mo(a)–B(1a)	2.21(2)
Mo–B(2)	2.21(2)	Mo(a)–B(2a)	2.26(2)	Mo–B(3)	2.36(2)	Mo(a)–B(3a)	2.33(2)
Mo–C(8)	2.42(2)	Mo(a)–C(8a)	2.38(1)	Mo–C(9)	2.34(2)	Mo(a)–C(9a)	2.31(1)
Fe(1)–Fe(2)	2.590(3)	Fe(1a)–Fe(2a)	2.580(2)	Fe(1)–C(01)	1.72(2)	Fe(1a)–C(01a)	1.77(2)
Fe(1)–C(02)	1.77(2)	Fe(1a)–C(02a)	1.79(2)	Fe(1)–C(03)	1.77(2)	Fe(1a)–C(03a)	1.80(2)
Fe(1)–C(1)	2.04(1)	Fe(1a)–C(1a)	2.02(1)	Fe(1)–B(2)	2.12(2)	Fe(1a)–B(1a)	2.16(2)
Fe(2)–C(04)	1.76(2)	Fe(2a)–C(04a)	1.78(2)	Fe(2)–C(05)	1.74(2)	Fe(2a)–C(05a)	1.80(2)
Fe(2)–C(06)	1.75(2)	Fe(2a)–C(06a)	1.82(2)	Fe(2)–C(1)	2.02(2)	Fe(2a)–C(1a)	2.04(1)
Fe(2)–B(1)	2.12(2)	Fe(2a)–B(2a)	2.16(2)	C(01)–O(1)	1.21(2)	C(01a)–O(1a)	1.17(2)
C(02)–O(2)	1.16(2)	C(02a)–O(2a)	1.14(2)	C(03)–O(3)	1.15(2)	C(03a)–O(3a)	1.12(2)
C(04)–O(4)	1.18(2)	C(04a)–O(4a)	1.12(2)	C(05)–O(5)	1.22(2)	C(05a)–O(5a)	1.14(2)
C(06)–O(6)	1.17(2)	C(06a)–O(6a)	1.15(2)	C(07)–O(7)	1.16(2)	C(07a)–O(7a)	1.13(2)
C(08)–O(8)	1.14(2)	C(08a)–O(8a)	1.12(2)	C(1)–C(2)	1.51(2)	C(1a)–C(2a)	1.50(2)
*Mean N–C	1.52	*Mean N(a)–C(a)	1.52	*Mean C–C	1.54	*Mean C(a)–C(a)	1.52
Fe(1)–Mo–Fe(2)	59.0(1)	Fe(1a)–Mo(a)–Fe(2a)	58.4(1)	Mo–Fe(1)–Fe(2)	60.1(1)	Mo(a)–Fe(1a)–Fe(2a)	60.8(1)
Mo–Fe(2)–Fe(1)	61.0(1)	Mo(a)–Fe(2a)–Fe(1a)	60.7(1)	Fe(1)–Mo–C(07)	90.7(5)	Fe(1a)–Mo(a)–C(07a)	93.2(4)
Fe(2)–Mo–C(07)	134.3(5)	Fe(2a)–Mo(a)–C(07a)	134.1(4)	Fe(1)–Mo–C(08)	132.3(5)	Fe(1a)–Mo(a)–C(08a)	133.0(4)
Fe(2)–Mo–C(08)	94.4(5)	Fe(2a)–Mo(a)–C(08a)	91.0(4)	C(07)–Mo–C(08)	81.5(6)	C(07a)–Mo(a)–C(08a)	84.0(5)
Fe(1)–Mo–C(1)	49.6(4)	Fe(1a)–Mo(a)–C(1a)	49.0(4)	Fe(2)–Mo–C(1)	49.6(4)	Fe(2a)–Mo(a)–C(1a)	49.4(4)
C(07)–Mo–C(1)	84.9(6)	C(07a)–Mo(a)–C(1a)	84.7(6)	C(08)–Mo–C(1)	82.7(6)	C(08a)–Mo(a)–C(1a)	84.2(5)
Mo–Fe(1)–C(01)	125.9(6)	Mo(a)–Fe(1a)–C(01a)	125.4(5)	Fe(2)–Fe(1)–C(01)	96.8(5)	Fe(2a)–Fe(1a)–C(01a)	95.9(5)
C(01–Fe(1)–C(1)	146.2(7)	C(01a)–Fe(1a)–C(1a)	146.0(6)	Mo–Fe(1)–C(02)	96.5(5)	Mo(a)–Fe(1a)–C(02a)	99.5(6)
Fe(2)–Fe(1)–C(02)	156.5(6)	Fe(2a)–Fe(1a)–C(02a)	158.5(5)	C(01)–Fe(1)–C(02)	99.6(8)	C(01a)–Fe(1a)–C(02a)	103.3(6)
C(02)–Fe(1)–C(1)	114.0(7)	C(02a)–Fe(1a)–C(1a)	110.7(6)	Mo–Fe(1)–C(03)	133.8(6)	Mo(a)–Fe(1a)–C(03a)	132.9(5)
Fe(2)–Fe(1)–C(03)	99.8(6)	Fe(2a)–Fe(1a)–C(03a)	95.6(5)	C(01)–Fe(1)–C(03)	95.6(9)	C(01a)–Fe(1a)–C(03a)	95.1(7)
C(02)–Fe(1)–C(03)	95.2(8)	C(02a)–Fe(1a)–C(03a)	92.3(7)	C(03)–Fe(1)–C(1)	85.6(7)	C(03a)–Fe(1a)–C(1a)	83.3(6)
Mo–Fe(1)–C(1)	49.0(4)	Mo(a)–Fe(1a)–C(1a)	49.8(4)	Fe(2)–Fe(1)–C(1)	50.0(4)	Fe(2a)–Fe(1a)–C(1a)	50.7(4)
Mo–Fe(2)–C(04)	124.1(5)	Mo(a)–Fe(2a)–C(04a)	125.8(5)	Fe(1)–Fe(2)–C(04)	105.9(5)	Fe(1a)–Fe(2a)–C(04a)	100.2(4)
Mo–Fe(2)–C(05)	95.8(5)	Mo(a)–Fe(2a)–C(05a)	95.5(6)	Fe(1)–Fe(2)–C(05)	151.8(5)	Fe(1a)–Fe(2a)–C(05a)	155.3(6)
C(04)–Fe(2)–C(05)	100.4(7)	C(04a)–Fe(2a)–C(05a)	99.5(7)	Mo-Fe(2)–C(06)	134.8(6)	Mo(a)–Fe(2a)–C(06a)	134.7(5)
Fe(1)–Fe(2)–C(06)	90.4(6)	Fe(1a)–Fe(2a)–C(06a)	96.8(5)	C(04)–Fe(2)–C(06)	95.8(8)	C(04a)–Fe(2a)–C(06a)	94.9(7)
C(05)–Fe(2)–C(06)	97.0(8)	C(05a)–Fe(2a)–C(06a)	96.2(7)	Mo–Fe(2)–C(1)	49.5(4)	Mo(a)–Fe(2a)–C(1a)	49.7(4)
Fe(1)–Fe(2)–C(1)	50.6(4)	Fe(1a)–Fe(2a)–C(1a)	50.1(3)	C(04)–Fe(2)–C(1)	156.5(6)	C(04a)–Fe(2a)–C(1a)	149.9(5)
C(05)–Fe(2)–C(1)	102.7(6)	C(05a)–Fe(2a)–C(1a)	110.4(7)	C(06)–Fe(2)–C(1)	85.3(7)	C(06a)–Fe(2a)–C(1a)	85.3(6)
Fe(1)–C(01)–O(1)	173.5(14)	Fe(1a)–C(01a)–O(1a)	175.1(14)	Fe(1)–C(02)–O(2)	177.5(14)	Fe(1a)–C(02a)–O(2a)	176.4(13)
Fe(1)–C(03)–O(3)	177.7(20)	Fe(1a)–C(03a)–O(3a)	178.4(14)	Fe(2)–C(04)–O(4)	176.7(14)	Fe(2a)–C(04a)–O(4a)	176.0(12)
Fe(2)–C(05)–O(5)	177.5(15)	Fe(2a)–C(05a)–O(5a)	177.2(15)	Fe(2)–C(06)–O(6)	174.7(16)	Fe(2a)–C(06a)–O(6a)	179.3(14)
Mo–C(07)–O(7)	172.0(15)	Mo(a)–C(07a)–O(7a)	171.9(13)	Mo–C(08)–O(8)	177.8(14)	Mo(a)–C(08a)–O(8a)	176.0(13)
Mean Mo–C(1)–Fe	81	Mean Mo(a)–C(1a)–Fe(a)	81	Fe(1)–C(1)–Fe(2)	79.4(5)	Fe(1a)–C(1a)–Fe(2a)	79.1(5)
Mo–C(1)–C(2)	136.6(11)	Mo(a)–C(1a)–C(2a)	133.2(10)	Mean Fe–C(1)–C(2)	129	Mean Fe(a)–C(1a)–C(2a)	131
Mo–B(1)–Fe(2)	74.4(5)	Mo(a)–B(2a)–Fe(2a)	73.4(5)	Mo-B(2)–Fe(1)	75.2(5)	Mo(a)–B(1a)–Fe(1a)	74.5(5)
*Mean C–N–C	109	*Mean C(a)–N(a)–C(a)	109	*Mean N–C–C	115	*Mean N(a)–C(a)–C(a)	116

* Parameter for the cation, $[NEt_4]^+$.

two iron atoms and the μ_3-CC_6H_4Me-4 moiety, is ligated by the η^5-$C_2B_9H_7Me_2$ *nido*-icosahedral fragment and two terminal CO groups. Each iron atom also carries three CO ligands. Evidently these groups undergo site exchange on the n.m.r. time-scale since, as mentioned above, only two CO resonances are seen, but these are of 3:1 relative intensity compared with the signals for the $Mo(CO)_2$ moiety.

As in previous structures of this type,[2b,e-h] the 'slippage' of the cage results in the metal atom (molybdenum) moving away from an axis through the centroid of the B(1)B(2)B(3)C(8)C(9) ring. This is accompanied by a 'folding' of the C_2B_3 face about the two atoms B(3) and C(9). These 'slip' and 'fold' distortions[7] have been defined in terms of three parameters: (*i*) a slip distance (Δ) from the perpendicular through the centroid of the non-bonded pentagonal B_5 girdle [Figure, B(4)—B(8)] and the metal atom, and (*ii*) fold angles θ and Φ representing the angles between the perpendicular through the centroid of the B(4)—B(8) ring and the planes defined by C(9)B(1)B(2)B(3) and by B(3)C(8)C(9). For (**10a**) these parameters are 0.17 Å, 1.4 and 0.5°, respectively. Whereas the slip distance is very similar to that for (**10b**) (0.19 Å) the fold angles are significantly different than those for (**10b**) (θ 0.7, Φ 0.5°).[2g]

The ^{11}B-$\{^1H\}$ n.m.r. spectrum of (**10a**) showed two very deshielded resonances at δ 47.8 and 59.0 p.p.m. which may be assigned to the two BFe groups. These resonances compare favourably with those in the ^{11}B-$\{^1H\}$ n.m.r. spectrum of (**10b**) at δ 45.1 and 55.9 p.p.m.[2g] Moreover, no ^1H-^{11}B coupling was observed on the BFe signals for (**10a**) in an ^{11}B spectrum.

The i.r. spectrum of (**11**) (Table 1) showed two CO stretches at 1 964vs and 1 865m cm^{-1}, and a weak BH band at 2 548 cm^{-1}. In the ^{13}C-$\{^1H\}$ n.m.r. spectrum (Table 2) there was no peak for an alkylidyne group, but signals due to the C_6H_4 fragment were apparent, as was a resonance at δ 80.0 p.p.m. assigned to the $BCH(C_6H_4Me$-4) moiety. This peak was broad due to unresolved ^{11}B-^{13}C coupling. In the ^{13}C-$\{^1H\}$ n.m.r. spectrum of (**3**), which also contains a $BCH(C_6H_4Me$-4) group, the resonance for the BCMo system occurs at δ 73.1 p.p.m., and is also broad.[3a] Only one CO resonance (δ 233.0 p.p.m.) is

observed in the room temperature ^{13}C-{^1H} n.m.r. spectrum of (**11**), indicating site exchange of the carbonyl groups. However, in a spectrum measured at −80 °C three broad peaks are seen at δ 234.7, 232.1, and 231.5 p.p.m. in accord with the presence of the $Mo(CO)_3$ group. The ^1H n.m.r. spectrum was informative. A resonance at δ 5.10 can be assigned to the $CH(C_6H_4Me\text{-}4)$ proton. This signal agrees well with those observed for this proton in the spectra of (**3**) (δ 5.01)[3a] and (**4**) (δ 5.95).[2b]

The ^{11}B-{^1H} n.m.r. spectrum of (**11**) shows a signal at δ 8.7 p.p.m. (Table 3) due to the $BCH(C_6H_4Me\text{-}4)$ nucleus. This resonance reveals no ^1H-^{11}B coupling in a ^{11}B n.m.r. spectrum. In the ^{11}B-{^1H} n.m.r. spectrum of (**3**) and (**4**) the corresponding signals are at δ 34.0 and 65.4 p.p.m., respectively. The differences in chemical shift for the $BCH(C_6H_4Me\text{-}4)$ group among these three species may be due to the boron nucleus being present in (**11**) in a ring of different size to that in (**3**) or (**4**). Moreover, whereas in (**11**) the molybdenum atom has an 18-electron shell, the complexes (**3**) and (**4**) are electronically unsaturated.

An ^{11}B-^{11}B two-dimensional COSY n.m.r. spectrum of (**11**) allowed the observation of four cross peaks associated with the signal at δ 8.7 p.p.m. This is in accord with the structure shown in which the central boron of the $\overline{CBBBC}$ pentagonal face is linked to the $CH(C_6H_4Me\text{-}4)$ group. The asymmetry of the two pairs of boron nuclei to which this boron is attached renders these four nuclei inequivalent; the asymmetry being introduced by the $CH(C_6H_4Me\text{-}4)$ moiety.

The spectroscopic data for (**11**) leave little doubt as to its formulation, and this is supported by the reactions described below. The mode of formation of (**11**) is of interest. As mentioned earlier, the reaction of the $[NEt_4]^+$ salt of (**1c**) with iron carbonyls affords a mixture of (**10b**) and (**12**).[2g] Other studies[2h] provide good evidence that a common precursor to both (**10b**) and (**12**) is a dimetal species $[WFe(\mu\text{-}CC_6H_4Me\text{-}4)(CO)_5(\eta^5\text{-}C_2B_9H_9Me_2)]^-$. The latter adds an iron carbonyl fragment and *via* loss of hydrogen forms (**10b**), while under the influence of CO, present in the reaction mixture, the dimetal compound affords (**12**). Based on previous results,[4a] it is likely that the initial reaction of $[Fe_2(CO)_9]$ with (**7**) affords a dimetal anionic complex $[MoFe(\mu\text{-}CC_6H_4Me\text{-}4)(CO)_5\{P(OMe)_3\}(\eta^5\text{-}C_2B_9H_9Me_2)]^-$ which releases $P(OMe)_3$ to give the unsaturated 32-valence electron species (**A**), shown in the accompanying Scheme. Structures of type (**B**) with B–H→metal linkages are well documented for species having W–W, W–Mo, W–Ru, W–Pt, and W–Ir bonds.[2,3b] The transformation from (**B**) to (**C**), a hydrido–metal complex, involves formal oxidative addition at the iron centre, a process recently established for iridium in a B–H→Ir species.[3b] Intermediate (**D**) is structurally related to complex (**12**), the structure of which has been established by *X*-ray diffraction.[2g] Under the influence of CO, present in solutions containing iron carbonyls, intermediate (**D**) could afford (**11**) with concomitant release of $[Fe(CO)_5]$. Compound (**10a**) might form *via* addition of an iron carbonyl fragment to (**C**) with loss of hydrogen. Thus (**C**) could be a common intermediate for both (**10a**) and (**11**). Interestingly, the transformation from a structure of type (**A**) (R = C_6H_4Me-2) into one of type (**D**) has recently been demonstrated.[2h]

The novel structure of the anion of (**11**) prompted protonation studies in an attempt to obtain a neutral species. As mentioned earlier, compounds (**10a**) and (**11**) are difficult to separate and so a mixture of the two species was protonated (HBF_4·Et_2O) in CH_2Cl_2 at −78 °C, and an excess of PMe_3 was added to stabilise any mononuclear molybdenum complex formed. This treatment led to the recovery of (**10a**) unchanged, and the formation of the two compounds $[Mo(CO)_3(L)\{\eta^5\text{-}C_2B_9H_8(CH_2C_6H_4Me\text{-}4)Me_2\}]$ [L = PMe_3 (**13a**) or CO (**13b**)]. If CO-saturated solutions of (**10a**) and (**11**) are protonated, compound (**13b**) is obtained in increased yield. However, under these conditions (**10a**) is not recovered due to formation of another product, discussed below.

Data for the compounds (**13**) are given in Tables 1—3 and are in accord with the structures shown. The i.r. spectrum (Table 1) of (**13a**) shows three CO stretching bands (2 028s, 1 963m, and 1 924vs cm^{-1}), as expected. The spectrum of (**13b**) also showed three CO absorptions (2 093vs, 2 034m, and 2 001s, br cm^{-1}) but the latter is very broad suggesting overlap of two peaks. In the ^{31}P-{^1H} n.m.r. spectrum of (**13a**) the resonance for the PMe_3 ligand occurs as a singlet at δ 12.2 p.p.m. The ^{11}B-{^1H} n.m.r. spectrum (Table 3) shows a signal at δ 9.7 p.p.m. assignable to the $BCH_2C_6H_4Me\text{-}4$ group. For (**13b**) the $BCH_2C_6H_4Me\text{-}4$ resonance is at δ 13.4 p.p.m. In the ^{11}B-{^1H} n.m.r. spectrum of (**6**) the corresponding peak is more deshielded at δ 28.9 p.p.m.[2e]

The ^1H n.m.r. spectra (Table 2) of the compounds (**13**) were informative. In addition to the resonances due to the $C_6H_4Me\text{-}4$ and CMe fragments, the spectrum of (**13a**) showed a doublet [*J*(PH) 10 Hz] at δ 1.92 for the Me groups of the PMe_3 ligand, and a broad singlet at δ 2.15 due to the CH_2 group of the $BCH_2C_6H_4Me\text{-}4$ moiety. In the spectrum of (**13b**) there was a corresponding signal at δ 2.18 These resonances compare favourably with that observed (δ 3.03) for the same group in (**6**).[2e] The ^{13}C-{^1H} n.m.r. spectral data for (**13a**) and (**13b**) also support the structural assignment. Characteristic peaks for the $BCH_2C_6H_4Me\text{-}4$ nuclei appear at δ 33.0 (**13a**) and 32.6 p.p.m. (**13b**), both signals being broad due to the proximity of boron nuclei. The corresponding peak in the spectrum of (**6**) occurs at δ 36.8 p.p.m. Moreover, the broad resonance at δ 80.0 p.p.m. due to the $BCH(C_6H_4Me\text{-}4)$ moiety in (**11**) is absent in the spectra of (**13a**) and (**13b**). The CO groups in (**13b**) evidently undergo fluxional behaviour since only one CO resonance is observed (δ 220.3 p.p.m.). The dynamic behaviour would involve rotation of the $Mo(CO)_4$ group about an axis through the molybdenum atom and the centroid of the pentagonal face of the cage. It is noteworthy that in the spectra of both complexes the CMe groups give rise to only two resonances (*C*Me and C*Me*, Table 3). This is in agreement with the symmetrical structure in which the $CH_2C_6H_4Me\text{-}4$ moiety is bonded to the central boron $\overline{CBBBC}$ of the pentagonal face of the cage. In addition, in (**13a**), for equivalence of the CMe fragments, the PMe_3 ligand must lie in a plane of symmetry, containing one CO and the BCH_2 unit, and which bisects the C–C bond in the face of the icosahedral fragment. This would account for the two CO resonances (δ 228.9 and 228.6 p.p.m., relative intensity 2:1) observed in the spectrum of (**13a**).

During protonation of mixtures of (**10a**) and (**11**) at −78 °C in CH_2Cl_2 solutions saturated with CO, the formation of (**13b**) is accompanied by formation of the trimetal complex $[MoFe_2(\mu\text{-}H)(\mu_3\text{-}CC_6H_4Me\text{-}4)(\mu\text{-}\sigma\text{:}\sigma'\text{:}\eta^5\text{-}C_2B_9H_7Me_2)(CO)_8]$ (**14**), and compound (**10a**) is not recovered. Presumably, if an excess of PMe_3 is present when the mixture is protonated, formation of $[PHMe_3][BF_4]$ is more rapid than protonation of (**10a**). Moreover, when pure samples of (**10a**) are protonated, (**14**) is obtained in good yield. The presence of the μ-H group in (**14**) was immediately revealed by the appearance of a peak at δ −24.98 in the ^1H n.m.r. spectrum (Table 2). Interestingly, a weak signal at δ −26.83 indicated that (**14**) was formed as a mixture of two isomers. Based on peak intensities, the second isomer is present only to the extent of 10—15%.

The ^{11}B-{^1H} n.m.r. spectrum of (**14**) revealed two diagnostic peaks (δ 46.2 and 58.7 p.p.m.) for the BFe groups, and these resonances showed no ^1H-^{11}B coupling in an ^{11}B spectrum. The presence of the second isomer was hard to detect, but a weak resonance at δ 41.4 p.p.m. may be due to such a species, the other BFe group signal overlapping the signal for the major isomer at δ 58.7 p.p.m.

In the ^{13}C-{^1H} n.m.r. spectrum of (**14**) the μ_3-C resonance is

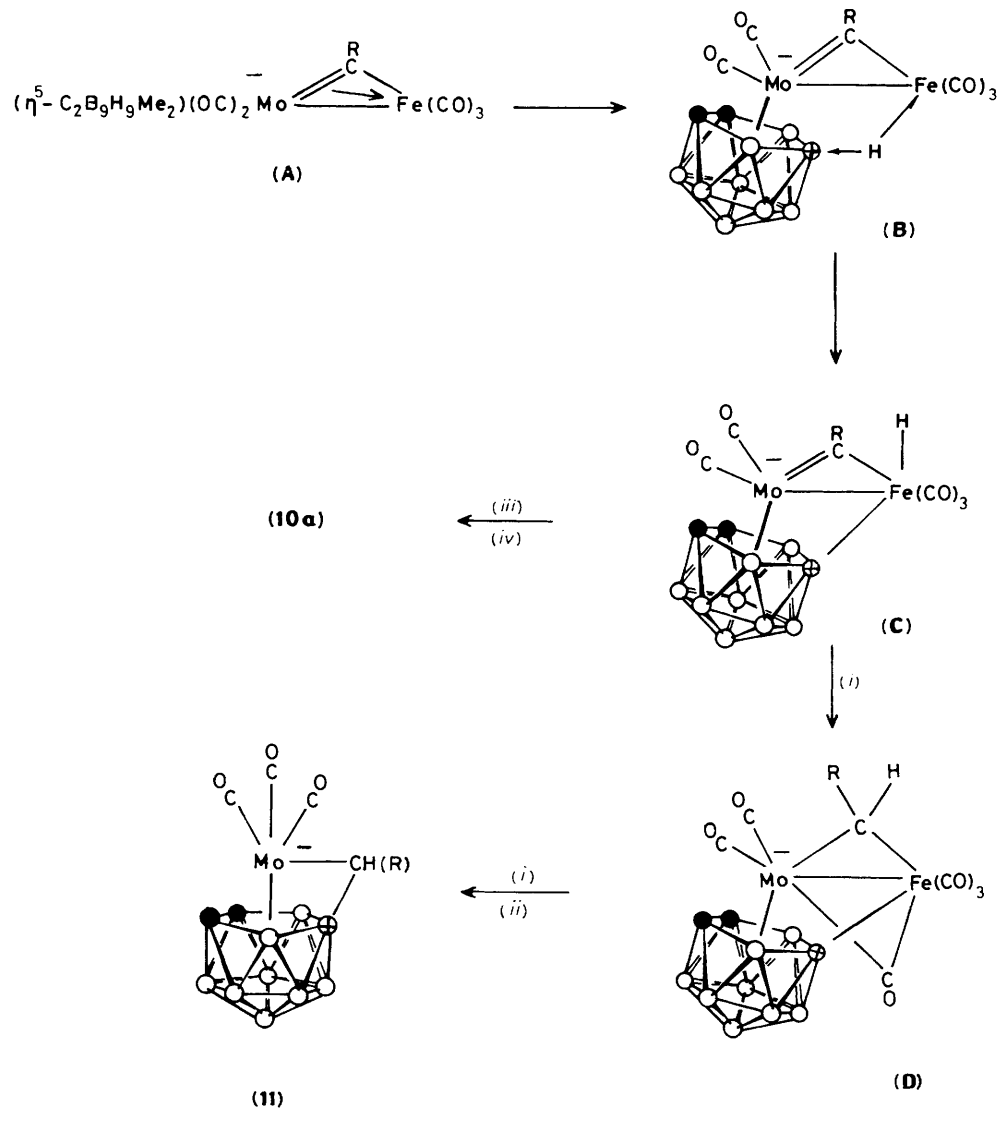

Scheme. R = C_6H_4Me-4. (*i*) +CO, (*ii*) −[$Fe(CO)_5$], (*iii*) $-H_2$, (*iv*) +$Fe(CO)_3$

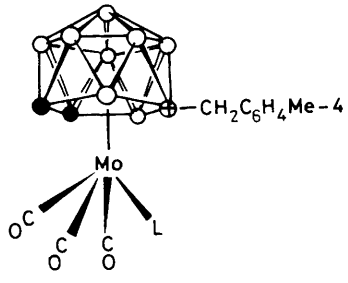

(13a) PMe_3

(13b) CO

at δ 312.6 p.p.m., very similar to that observed (314.0 p.p.m.) for (**10a**). The μ_3-C signal for the minor isomer was seen at δ 312.4 p.p.m. In the CO region of the spectrum of (**14**) there are two MoCO and six FeCO resonances (Table 2). Evidently, in contrast with (**10a**), the CO groups in (**14**) are not undergoing exchange on the n.m.r. time-scale. The data suggest a structure very similar to (**10a**) but with a Mo–Fe bond bridged by the hydrido ligand. This arrangement would introduce an asymmetry, giving rise to the six FeCO resonances. In support of this inference, the three CO resonances at δ 210.8, 210.5, and 206.3 p.p.m. are broad suggesting incipient fluxional behaviour for an $Fe(CO)_3$ fragment on the unbridged side of the metal triangle.

The presence of two isomers is readily understood in terms of the hydride bridging a Mo–Fe rather than the Fe–Fe bond. As a result of the presence of the two B–Fe σ bonds, the CMe groups are directed towards one side of the metal triangle rendering each Mo–Fe bond asymmetric with respect to the cage. Therefore, the two isomers of (**14**) could involve the hydride bridging one or other of the Mo–Fe bonds. For a structure in which the hydrido group bridges the Fe–Fe bond two isomers are not possible. In conclusion, it is interesting to note that protonation of (**10b**) and structurally related tungsten–di-iron compounds was not successful.[2g,h]

The results described in this paper clearly show that the salt (**7**) has a rich chemistry. The transformation of the terminal alkylidyne group in (**7**) into the alkyl substituent on the cage in the complexes (**13**) is without precedent. Moreover, it is evident that (**7**) shows distinct differences in reactivity compared with salts of the anions (**1**).

Experimental

Experiments were carried out using Schlenk-tube techniques, under a dry oxygen-free nitrogen atmosphere. Light petroleum refers to that fraction of b.p. 40—60 °C, and all solvents were freshly distilled over appropriate drying agents prior to use. Chromatography columns (3 × 15 cm) were of alumina (Brockman Activity II) or Florisil (100—200 mesh). The compounds $[AuCl(PPh_3)]$,[8] $[Rh(cod)(PPh_3)_2][PF_6]$,[9] and $[NHMe_3][7,8\text{-}C_2B_9H_{10}Me_2]$[10] were prepared by literature methods, and $[Mo(\equiv CC_6H_4Me\text{-}4)Cl(CO)\{P(OMe)_3\}_3]$ was obtained by the route previously reported for the CPh analogue.[11] The $HBF_4{\cdot}Et_2O$ used for protonation was from Aldrich (85% HBF_4). Analytical and other data for the new compounds are given in Table 1. The instrumentation used for the spectroscopic measurements has been described in previous parts of this series.[2,3]

Synthesis of $[NEt_4][Mo(\equiv CC_6H_4Me\text{-}4)(CO)\{P(OMe)_3\}(\eta^5\text{-}C_2B_9H_9Me_2)]$.—A solution of $Na_2[7,8\text{-}C_2B_9H_9Me_2]$ was prepared by refluxing $[NHMe_3][7,8\text{-}C_2B_9H_{10}Me_2]$ (1.45 g, 6.54 mmol) and NaH (1.5 g, from a 60% dispersion in mineral oil) in thf (60 cm^3). The resulting solution was decanted. Additional thf (10 cm^3) was used to wash the NaH residue, and the washings were added to the decanted solution of $Na_2[7,8\text{-}C_2B_9H_9Me_2]$. The latter was then treated with $[Mo(\equiv CC_6H_4\text{-}Me\text{-}4)Cl(CO)\{P(OMe)_3\}_3]$ (4.15 g, 6.54 mmol) dissolved in thf (60 cm^3), and the mixture was stirred for 2 h, after which time $[NEt_4]Cl$ (2.16 g, 13 mmol) was added. Stirring was continued (1 h) and then the solvent was removed *in vacuo*. The residue was treated with CH_2Cl_2 (60 cm^3), and filtered through a Celite pad (2 × 3 cm). The excess $[NEt_4]Cl$ which remained, and the Celite pad, were washed with additional CH_2Cl_2 (2 × 15 cm^3), and the washings were combined with the filtrate. The volume of the resulting solution was reduced *in vacuo* to *ca.* 20 cm^3 and chromatographed on alumina at −40 °C. Elution with CH_2Cl_2 gave a red-orange eluate. Removal of solvent *in vacuo* afforded an oily residue. Repeated washing with Et_2O (6 × 20 cm^3) gave red *microcrystals* of $[NEt_4][Mo(\equiv CC_6H_4Me\text{-}4)(CO)\{P(OMe)_3\}(\eta^5\text{-}C_2B_9H_9Me_2)]$ (**7**) (2.25 g).

Reactions of $[NEt_4][Mo(\equiv CC_6H_4Me\text{-}4)(CO)\{P(OMe)_3\}(\eta^5\text{-}C_2B_9H_9Me_2)]$.—(*i*) A thf (15 cm^3) solution of (**7**) (0.40 g, 0.62 mmol) was treated with $[AuCl(PPh_3)]$ (0.31 g, 0.62 mmol) and KPF_6 (0.17 g, 0.93 mmol), and the mixture was stirred at room temperature for 1 h. Solvent was removed *in vacuo*, and the residue was extracted with Et_2O (5 × 20 cm^3). The extracts were reduced in volume *in vacuo* to *ca.* 15 cm^3, then CH_2Cl_2 (5 cm^3) was added to give a 3:1 Et_2O–CH_2Cl_2 solution which was chromatographed at room temperature on a Florisil column. Elution with the same solvent mixture yielded a red eluate, which after removal of solvent *in vacuo* gave red *microcrystals* of $[MoAu(\mu\text{-}CC_6H_4Me\text{-}4)(CO)\{P(OMe)_3\}(PPh_3)(\eta^5\text{-}C_2B_9H_9Me_2)]$ (**8a**) (0.29 g).

(*ii*) A CH_2Cl_2 (20 cm^3) solution of (**7**) (0.40 g, 0.62 mmol) was treated with solid $[Rh(cod)(PPh_3)_2][PF_6]$ (0.55 g, 0.62 mmol), and the mixture was stirred for 20 min. Solvent was removed *in vacuo*, and the residue was washed (2 × 20 cm^3) with a CH_2Cl_2–light petroleum (1:3) mixture. The washed solid was dissolved in CH_2Cl_2 (10 cm^3) and chromatographed on alumina at −30 °C. Elution with the same solvent gave a brown eluate from which solvent was removed *in vacuo*. The residue was washed with CH_2Cl_2–light petroleum (20 cm^3, 1:9) affording brown *microcrystals* of $[MoRh(\mu\text{-}CC_6H_4Me\text{-}4)(\mu\text{-}CO)\{P(OMe)_3\}(PPh_3)_2(\eta^5\text{-}C_2B_9H_9Me_2)]$ (**9a**) (0.39 g).

(*iii*) (a) A sample of $[Fe_2(CO)_9]$ (1.36 g, 3.74 mmol) was added to a thf (30 cm^3) solution of (**7**) (0.60 g, 0.94 mmol) and the mixture was stirred for 12 h at room temperature. Solvent was removed *in vacuo*, and the residue was dissolved in CH_2Cl_2–light petroleum (20 cm^3, 3:1) and chromatographed on alumina at −30 °C. Elution with the same solvent mixture afforded a fast green band identified (i.r.) as $[Fe_3(CO)_{12}]$. This was followed by a broad olive-brown fraction containing the desired products, and a purple eluate containing $[NEt_4][Fe_3(\mu\text{-}H)(CO)_{11}]$ identified by i.r. Care must be taken to avoid contamination of the olive-brown eluate by either $[Fe_3(CO)_{12}]$ or $[NEt_4][Fe_3(\mu\text{-}H)(CO)_{11}]$, otherwise further chromatography is necessary. Removal of solvent *in vacuo* from the olive-brown eluate gives an *ca.* 1:1 mixture (0.32 g) of $[NEt_4][MoFe_2(\mu_3\text{-}CC_6H_4Me\text{-}4)(\mu\text{-}\sigma:\sigma':\eta^5\text{-}C_2B_9H_7Me_2)(CO)_8]$ (**10a**) and $[NEt_4][Mo\{\sigma,\eta^5\text{-}CH(C_6H_4Me\text{-}4)C_2B_9H_8Me_2\}(CO)_3]$ (**11**). Complex (**10a**) was obtained pure in the following manner. The mixture was dissolved in CH_2Cl_2 (15 cm^3) in a wide-bore Schlenk-tube, and light petroleum (40 cm^3) was layered upon the CH_2Cl_2 without mixing. After 24 h crystals of (**10a**) appeared, covered by an oil containing (**11**). The volume was reduced to *ca.* 15 cm^3, and CH_2Cl_2 (*ca.* 3—5 cm^3) was added. This treatment removed the oily material and allowed recovery of brown crystals of (**10a**) (0.14 g). Removal of solvent *in vacuo* gave (**11**) (0.18 g) as an oily residue containing *ca.* 10% of (**10a**), as estimated by n.m.r.

(b) The reagent (**7**) (0.60 g, 0.94 mmol) and $[Fe_2(CO)_9]$ (1.36 g, 3.74 mmol) were dissolved in thf (30 cm^3) and the mixture was stirred for 12 h at ambient temperatures. Isolation of the product mixture (**10a**) and (**11**) was accomplished as described above. The mixture of the two complexes was treated with CH_2Cl_2 (30 cm^3) and the solution was cooled to −78 °C. With a micro-syringe, 90 μl (*ca.* 0.50 mmol) of $HBF_4{\cdot}Et_2O$ solution was added. After 2 min, PMe_3 (0.59 mmol) were added, and the mixture was stirred for 30 min and warmed to room temperature. After removing solvent *in vacuo*, a dark orange residue was obtained. The residue was extracted (2 × 20 cm^3) with Et_2O–light petroleum (2:1), and the extracts were chromatographed on Florisil at −40 °C. Elution with the same solvent mixture afforded three bands on the column. The first brown-orange eluate was discarded since it contained decomposed material. The second yellow-orange eluate, after removal of solvent *in vacuo*, gave tan *microcrystals* of $[Mo(CO)_4\{\eta^5\text{-}C_2B_9H_8(CH_2C_6H_4Me\text{-}4)Me_2\}]$ (**13b**) (0.04 g). The third tan coloured band was eluted with Et_2O–thf (7:3) and after removal of solvent *in vacuo* gave tan *microcrystals* of $[Mo(CO)_3(PMe_3)\{\eta^5\text{-}C_2B_9H_8(CH_2C_6H_4Me\text{-}4)Me_2\}]$ (**13a**) (0.06 g). The residue from which (**13a**) and (**13b**) were extracted prior to chromatography was dissolved in CH_2Cl_2 (15 cm^3) and chromatographed at −40 °C, eluting with the same solvent. One olive-brown eluate was collected, and after removal of solvent *in vacuo* afforded brown *microcrystals* of (**10a**) (0.11 g).

(c) Compound (**7**) (0.60 g, 0.94 mmol) and $[Fe_2(CO)_9]$ (1.36 g, 3.74 mmol) were stirred in thf (30 cm^3) for 12 h at room temperature. The mixture of (**10a**) and (**11**) was isolated as in (a) above, and dissolved in CH_2Cl_2 (30 cm^3) cooled to −78 °C. The solution was saturated with a stream of CO (5 min), and then treated with $HBF_4{\cdot}Et_2O$ (0.50 mmol). The CO bubbling was maintained for 30 min. The mixture was slowly warmed to room temperature, solvent was removed *in vacuo*, and the dark yellow residue was dissolved in Et_2O–light petroleum (20 cm^3, 1:1) and chromatographed on Florisil at −40 °C. Two bands developed on the column. The first yellow-brown band was removed with the same solvent mixture. Removal of solvent *in vacuo* gave a yellow-brown residue which was further purified by dissolving in Et_2O–light petroleum (10 cm^3, 2:1) and

chromatographing at −60 °C on alumina (3 × 10 cm column), eluting with Et_2O–light petroleum (2:1). Removal of solvent *in vacuo* gave yellow-brown *microcrystals* of $[MoFe_2(\mu\text{-}H)(\mu_3\text{-}CC_6H_4Me\text{-}4)(\mu\text{-}\sigma\text{:}\sigma'\text{:}\eta^5\text{-}C_2B_9H_7Me_2)(CO)_8]$ (**14**) (0.14 g). The second band on the Florisil column was eluted with Et_2O. Removal of solvent *in vacuo* gave tan *microcrystals* of (**13b**) (0.09 g).

Compound (**14**) (0.34 g) was also obtained (70%) by protonation of a pure sample of (**10a**) (0.06 g, 0.07 mmol) in CH_2Cl_2 (15 cm^3) at −78 °C with $HBF_4{\cdot}Et_2O$ (*ca.* 0.10 mmol).

Crystal-structure Determination.—Crystals of (**10a**) were grown as dark brown rhomboids from a CH_2Cl_2 solution containing (**10a**) and (**11**) by layering light petroleum on the CH_2Cl_2 and leaving the system at room temperature for several days. The crystals were washed free of (**11**) with a small amount (*ca.* 2 cm^3) of CH_2Cl_2 after *ca.* 70% of the solvent mixture had been removed. The crystal chosen for study had dimensions *ca.* 0.55 × 0.35 × 0.40 mm, and was sealed under nitrogen in a Lindemann tube. Diffracted intensities were collected (2θ scans) in the range $3 \leqslant 2\theta \leqslant 50°$ at 200 K on a Nicolet *P3m* four-circle diffractometer. Of 14 450 unique intensities, 5 455 had $F \geqslant 4\sigma(F)$, where $\sigma(F)$ is the standard deviation in F based on counting statistics. Only these data were used in the final refinement of the structure, after all the data had been corrected for Lorentz and polarisation effects, and an empirical correction had been applied for *X*-ray absorption.[12]

Crystal data. $[C_8H_{20}N]^+[C_{20}H_{20}B_9Fe_2MoO_8]^-$, M = 823.55, monoclinic, a = 20.118(6), b = 12.447(4), c = 29.236(9) Å, β = 99.79(2)°, U = 7 215(4) $Å^3$, D_c = 1.52 g cm^{-3},

Table 5. Atomic positional parameters (fractional co-ordinates, × 10^4) with standard deviations in parentheses for (**10a**)

Molecule 1				Molecule 2			
Atom	*x*	*y*	*z*	Atom	*x*	*y*	*z*
Mo	4 766(1)	1 829(1)	1 008(1)	Mo(a)	9 604(1)	856(1)	946(1)
Fe(1)	3 501(1)	1 829(2)	1 147(1)	Fe(1a)	9 633(1)	109(2)	1 796(1)
Fe(2)	4 440(1)	2 633(2)	1 768(1)	Fe(2a)	8 524(1)	904(2)	1 351(1)
C(1)	4 151(7)	3 063(10)	1 098(5)	C(1a)	9 078(6)	−364(10)	1 188(5)
C(2)	3 999(7)	4 161(11)	890(5)	C(2a)	8 858(7)	−1 454(10)	1 003(5)
C(3)	4 353(7)	5 074(11)	1 066(5)	C(3a)	8 262(7)	−1 597(11)	679(5)
C(4)	4 277(7)	6 049(12)	859(5)	C(4a)	8 121(7)	−2 544(13)	456(5)
C(5)	3 838(8)	6 176(11)	436(5)	C(5a)	8 536(7)	−3 439(11)	526(5)
C(51)	3 784(8)	7 251(12)	174(6)	C(51a)	400(8)	−4 452(11)	250(5)
C(6)	3 478(8)	5 289(12)	241(5)	C(6a)	9 141(7)	−3 322(12)	853(5)
C(7)	3 572(8)	4 304(14)	458(6)	C(7a)	9 280(6)	−2 365(11)	1 092(5)
C(9)	5 576(7)	817(13)	1 494(6)	C(8a)	10 168(6)	2 417(10)	736(4)
C(91)	6 224(8)	1 410(15)	1 668(8)	C(81a)	10 459(8)	2 271(13)	292(5)
C(8)	5 450(8)	241(13)	991(5)	C(9a)	10 551(6)	1 849(11)	1 232(5)
C(81)	5 902(8)	313(15)	635(7)	C(91a)	11 200(7)	1 245(13)	1 248(6)
B(1)	4 802(9)	1 056(13)	1 694(5)	B(2a)	9 209(7)	2 233(13)	1 326(5)
B(3)	4 577(8)	1(13)	822(6)	B(3a)	9 348(8)	2 639(13)	748(6)
B(2)	4 186(8)	520(12)	1 264(6)	B(1a)	9 955(8)	1 679(14)	1 612(6)
B(4)	4 484(9)	−232(13)	1 795(7)	B(4a)	9 721(8)	2 955(14)	1 737(6)
B(5)	5 385(10)	8(15)	1 949(7)	B(5a)	9 309(9)	3 592(13)	1 196(6)
B(6)	5 740(10)	−533(17)	1 479(7)	B(6a)	9 936(9)	3 718(15)	852(7)
B(7)	5 132(9)	−1 057(13)	1 045(7)	B(7a)	10 692(9)	3 241(14)	1 151(6)
B(8)	4 301(9)	−890(13)	1 225(6)	B(8a)	10 569(9)	2 690(14)	1 698(6)
B(9)	5 052(12)	−1 188(16)	1 628(8)	B(9a)	10 174(9)	3 940(15)	1 473(6)
C(01)	3 164(8)	985(15)	1 512(6)	C(01a)	9 657(7)	905(12)	2 300(6)
C(02)	3 148(8)	1 256(12)	607(6)	C(02a)	10 443(8)	−522(12)	1 885(5)
C(03)	2 879(9)	2 840(15)	1 133(7)	C(03a)	9 247(8)	−1 030(12)	2 021(5)
C(04)	4 424(8)	1 889(13)	2 278(6)	C(04a)	8 351(7)	1 881(12)	1 758(5)
C(05)	5 186(9)	3 357(14)	1 930(5)	C(05a)	7 955(7)	1 360(13)	844(7)
C(06)	3 889(10)	3 639(15)	1 889(6)	C(06a)	7 962(8)	−110(13)	1 524(6)
C(07)	4 457(8)	2 102(12)	319(6)	C(07a)	10 221(7)	−366(13)	772(5)
C(08)	5 410(8)	3 028(13)	926(6)	C(08a)	9 031(7)	504(11)	328(5)
O(1)	2 867(6)	444(9)	1 756(4)	O(1a)	9 665(5)	1 365(8)	2 651(4)
O(2)	2 924(6)	844(11)	260(5)	O(2a)	10 955(6)	−934(10)	1 965(4)
O(3)	2 483(7)	3 507(10)	1 111(7)	O(3a)	8 992(6)	−1 728(10)	2 161(3)
O(4)	4 420(6)	1 433(9)	2 633(4)	O(4a)	8 204(5)	2 475(9)	2 012(3)
O(5)	5 691(6)	3 895(9)	2 046(4)	O(5a)	7 576(5)	1 623(10)	531(4)
O(6)	3 527(7)	4 285(10)	2 006(4)	O(6a)	7 613(6)	−757(9)	1 634(4)
O(7)	4 214(7)	2 302(10)	−59(4)	O(7a)	10 517(5)	−1 102(8)	707(4)
O(8)	5 777(6)	3 714(10)	895(4)	O(8a)	8 688(5)	276(9)	−2(4)
N(1)	7 347(5)	5 831(8)	1 719(4)	N(1a)	2 170(6)	6 840(10)	1 435(4)
Cn(1)	7 178(9)	6 087(11)	2 180(5)	Cn(1a)	2 933(8)	6 684(19)	1 553(8)
Cn(2)	7 262(10)	7 267(12)	2 330(6)	Cn(2a)	3 295(10)	7 262(20)	1 962(7)
Cn(3)	6 920(7)	6 546(12)	1 328(5)	Cn(3a)	1 833(8)	6 614(14)	1 843(6)
Cn(4)	6 169(9)	6 363(14)	1 268(6)	Cn(4a)	1 947(10)	5 463(15)	2 031(7)
Cn(5)	7 229(7)	4 675(11)	1 642(5)	Cn(5a)	1 887(10)	6 119(14)	1 036(7)
Cn(6)	7 337(9)	4 257(14)	1 166(6)	Cn(6a)	1 121(10)	6 219(17)	822(9)
Cn(7)	8 071(6)	6 157(10)	1 688(5)	Cn(7a)	2 026(8)	8 045(11)	1 309(5)
Cn(8)	8 624(7)	5 614(14)	2 058(5)	Cn(8a)	2 282(8)	8 387(14)	876(6)

$Z = 8$, $F(000) = 3\,343.5$, space group $P2_1/c$, Mo-K_α X-radiation (graphite monochromator), $\bar{\lambda} = 0.710\,69$ Å, μ(Mo-K_α) = 18.19 cm^{-1}.

Structure solution and refinement. The structure was solved by heavy-atom methods; all non-hydrogen atoms were located from difference Fourier calculations and were refined anisotropically. Final refinement, by blocked, full-matrix least-squares techniques, was performed on a DEC μVax II computer with the SHELXTL-plus system of programs.[12] As discussed earlier, the salt (**10a**) crystallises with two independent configurations for the anion in the asymmetric unit. All hydrogen atoms were incorporated at calculated positions (C–H 0.96, B–H 1.10 Å) with tied isotropic thermal parameters (related to the U_{eq} for the atom to which they were attached). A weighting scheme of the form $w = [\sigma^2(F_o) + g|F_o|^2]^{-1}$, where $g = 0.0005$, was applied. The final difference density synthesis showed no peaks $> \pm 1.5$ e $Å^{-3}$. Scattering factors with corrections for anomalous dispersion, included in the programs,[12] were from ref. 13. Refinement converged at $R = 0.067$ ($R' = 0.068$). Atomic co-ordinates are listed in Table 5.

Additional material available from the Cambridge Crystallographic Data Centre comprises H-atom co-ordinates, thermal parameters, and remaining bond lengths and angles.

Acknowledgements

We thank the U.S.A.F. Office of Scientific Research for support under Grant 86-0125.

References

1 Part 85, S. J. Davies and F. G. A. Stone, preceding paper.
2 (*a*) M. Green, J. A. K. Howard, A. P. James, C. M. Nunn, and F. G. A. Stone, *J. Chem. Soc., Dalton Trans.*, 1987, 61; (*b*) M. Green, J. A. K. Howard, A. N. de M. Jelfs, O. Johnson, and F. G. A. Stone, *ibid.*, p. 73; (*c*) M. Green, J. A. K. Howard, A. P. James, A. N. de M. Jelfs, C. M. Nunn, and F. G. A. Stone, *ibid.*, p. 81; (*d*) J. A. K. Howard, A. P. James, A. N. de M. Jelfs, C. M. Nunn, and F. G. A. Stone, *ibid.*, p. 1221; (*e*) M. J. Attfield, J. A. K. Howard, A. N. de M. Jelfs, C. M. Nunn, and F. G. A. Stone, *ibid.*, p. 2219; (*f*) F-E. Baumann, J. A. K. Howard, O. Johnson, and F. G. A. Stone, *ibid.*, p. 2661; (*g*) F-E. Baumann, J. A. K. Howard, O. Johnson, and F. G. A. Stone, *ibid.*, p. 2917; (*h*) F-E. Baumann, J. A. K. Howard, R. J. Musgrove, P. Sherwood, and F. G. A. Stone, *ibid.*, 1988, 1879, 1891; (*i*) D. D. Devore, J. A. K. Howard, J. C. Jeffery, M. U. Pilotti, and F. G. A. Stone, *ibid.*, 1989, 303.
3 (*a*) M. Green, J. A. K. Howard, A. P. James, A. N. de M. Jelfs, C. M. Nunn, and F. G. A. Stone, *J. Chem. Soc., Chem. Commun.*, 1985, 1778; (*b*) F-E. Baumann, J. A. K. Howard, R. J. Musgrove, P. Sherwood, M. A. Ruiz, and F. G. A. Stone, *ibid.*, 1987, 1881.
4 (*a*) M. E. Garcia, J. C. Jeffery, P. Sherwood, and F. G. A. Stone, *J. Chem. Soc., Dalton Trans.*, 1987, 1209; (*b*) M. E. Garcia, N. H. Tran-Huy, J. C. Jeffery, P. Sherwood, and F. G. A. Stone, *ibid.*, p. 2201; (*c*) M. E. Garcia, J. C. Jeffery, P. Sherwood, and F. G. A. Stone, *ibid.*, p. 2431, 2443; (*d*) S. J. Dossett, A. F. Hill, J. C. Jeffery, F. Marken, P. Sherwood, and F. G. A. Stone, *ibid.*, p. 2453.
5 J. A. Abad, L. W. Bateman, J. C. Jeffery, K. A. Mead, H. Razay, F. G. A. Stone, and P. Woodward, *J. Chem. Soc., Dalton Trans.*, 1983, 2075.
6 J. A. Abad, E. Delgado, M. E. Garcia, M. J. Grosse-Ophoff, I. J. Hart, J. C. Jeffery, M. S. Simmons, and F. G. A. Stone, *J. Chem. Soc., Dalton Trans.*, 1987, 41.
7 D. M. P. Mingos, M. I. Forsyth, and A. J. Welch, *J. Chem. Soc., Dalton Trans.*, 1978, 1363.
8 F. G. Mann, A. F. Wells, and D. Purdie, *J. Chem. Soc.*, 1937, 1828.
9 R. R. Schrock and J. A. Osborn, *J. Am. Chem. Soc.*, 1971, **93**, 2397.
10 M. F. Hawthorne, D. C. Young, P. M. Garrett, D. A. Owen, S. G. Schwerin, F. N. Tebbe, and P. A. Wegner, *J. Am. Chem. Soc.*, 1968, **90**, 862.
11 A. Mayr, A. M. Dorries, G. A. McDermott, and D. Van Eugen, *Organometallics*, 1986, **5**, 1504.
12 G. M. Sheldrick, University of Göttingen, 1987; Nicolet XRD Corporation, Madison, Wisconsin, U.S.A.
13 'International Tables for *X*-Ray Crystallography,' Kynoch Press, Birmingham, 1974, vol. 4.

Received 11*th May* 1988; *Paper* 8/01852I